

Structure of Triads in Geostrophic Turbulence

M. Yu. Reshetnyak

*Schmidt Institute of Physics of the Earth, Russian Academy of Sciences,
Bol'shaya Gruzinskaya ul. 10, Moscow, 123995 Russia
e-mail: m.reshetnyak@gmail.com*

Received September 3, 2008; in final form, October 30, 2008

Abstract—The interaction between Fourier waves, which results in energy transfer over the spectrum, has been considered using the Boussinesq model in a plane layer during rapid rotation as an example. It has been indicated that the wave triangle spectrum strongly differs on the scales shorter (longer) than the scale of a cyclonic turbulence leading mode.

PACS numbers: 91.25.Cw

DOI: 10.1134/S0016793209040173

1. INTRODUCTION

Energy transfer in the spectral space has been studied in different fields of physics. Hydrodynamics is legally considered to be one of the first such regions [Lesieur, 1990]. The possibility of energy transfer from large to small scales forms the basis for the Kolmogorov theory, which postulates the existence of a self-similar region in the wave space (the so-called inertial interval) with a constant energy flux from one wavenumber to another and with absent dissipation and external field work in this region (for more detail, see [Frisch, 1995]). According to the model, for homogeneous and isotropic turbulence, energy is transferred from slightly larger vortices to slightly smaller ones. When more complex systems (e.g., thermal turbulence or magnetic field problems) are considered, the concept of inertial interval becomes incorrect in the strict sense of the word since the work of forces is already nonzero on almost all scales. Moreover, energy transfer can reverse, and the so-called inverse energy cascade from small scales to large ones can originate [Kraichnan and Montgomery, 1980] as in the case of two-dimensional turbulence, the properties of which are close to those of rotating and magnetic turbulence (for more detail, see the α -effect theory in [Krause and Rädler, 1980]). It turns out that a simplified concept of a serial energy transfer between scales is only a rough approximation in many cases even for the problems of convection with forcing on a certain scale: the considered interaction between Fourier modes indicates that the structure of a wave triangle—a dependence of a result on a spectral range—is very complex [Alexakis et al., 2007]. Even if we assume that the energy is locally transferred over the spectrum from a mode with wavenumber $Q = |\mathbf{q}|$ to a mode with $K = |\mathbf{k}|$, when $P \sim K$, the amplitude of the third triad harmonic $P(\mathbf{p} + \mathbf{q} + \mathbf{k} = 0)$ can substantially differ from P and Q . If $P \sim Q$

$\sim K$, the triad coupling is said to be local. If $P \ll Q$ (or $P \gg Q$), it is said that energy is locally transferred due to nonlocal interaction. The calculations indicate that all models, reproducing a spectrum with the exponent close to that predicted by Kolmogorov ($-5/3$), generally simultaneously interact with a forcing scale, which corresponds to nonlocal coupling according to the classification proposed above. This is equivalent to deformation of small vortices by large ones.

When rotation is introduced, this leads to a substantial reconstruction of fluxes in the physical and wave spaces. The Coriolis force itself does not deliver work; nevertheless, the amplitude of large-scale fluxes can increase because the conditions are formed for an inverse energy cascade, which is observed in direct calculations [Hossain, 1994] and was predicted theoretically [McComb, 1992]. As a result, the exponent of the kinetic energy spectrum also increases from $-5/3$ to -2 [Zhou, 1995; Constantin, 2002]. This change is related to blocking of energy transfer over the spectrum [Zhou, 1995].

The conditions for the appearance of cyclonic convection with high vertical velocities originate when we pass to the problem with thermal convection, when the equation for temperature and the buoyancy force are added. In the physical space, the problem has already been sufficiently studied in the works devoted to the geodynamo. Rapid rotation results in the appearance of equilibrium between the Coriolis force and pressure gradient (the geostrophic balance) [Pedlosky, 1987]: $l_z \times \mathbf{V} \sim \nabla p$, from which it follows that the field gradients along the axis of rotation (\mathbf{z}) are small:

$\frac{\partial \mathbf{V}}{\partial z} \sim 0$.¹ Cyclones (anticyclones), extended along the

¹ Note that we mean the balance of the Coriolis force potential component.

axis of rotation, originate. If we consider the Earth's liquid core and decrease the amplitude of heat sources to the level at the convection origination onset, the diameter (d_c) of such cyclones will be five orders of magnitude as small as the cyclone height. A cluster of such cyclones actually exists in the wave space because convection in the Earth's core is turbulent (the Reynolds number reaches $Re \sim 10^9$); however, the geostrophic balance exists for at least the first three–four orders with respect to k according to the estimated orders of magnitude. This is substantially larger than the range of the geomagnetic field spectrum and should be taken into account when the dynamo models are constructed.

The appearance of the Coriolis force is also of importance for the dynamics of energy transfer in the wave space. Previously, the nonlinear term, which was of the same order of magnitude as the pressure gradient, easily transferred energy over the spectrum (e.g., due to the vortical part of the nonlinear term). When the Coriolis force was found out, the following situation became possible: pressure compensates the potential component of the Coriolis force. The vortical component of the Coriolis force blocks energy transferred by the nonlinear term. As a result, the spectrum becomes steeper. Such a situation is observed on small scales ($l \ll d_c$). On large scales ($l \gg d_c$), the system can be in the state of statistical equilibrium: dissipation is almost absent, and the energy transfer between the scales is negligible.

Below, we will consider the energy fluxes and the triad structure in the wave space for the Navier–Stokes equation for the regimes typical of models of convection in the Earth's liquid core, compare these characteristics with those in the regimes without rotation, and consider the degree of quantitative correspondence with several phenomenological models of turbulence mentioned above.

2. CONVECTION EQUATIONS

We now consider thermal convection of incompressible fluid $\nabla \cdot \mathbf{V} = 0$ in a rectangular box rotating about the vertical axis \mathbf{z} at angular velocity Ω . Having introduced the κ/L , L^2/κ , and $\rho\kappa^2/L^2$ units for velocity \mathbf{V} , time t , and pressure P , respectively (where L is the unit of length, κ is the coefficient of molecular thermal conductivity, and ρ is the substance density), we write the set of dynamo equations in Cartesian coordinates (x, y, z) in the form:

$$\begin{aligned} & EPr^{-1} \left[\frac{\partial \mathbf{V}}{\partial t} - \mathbf{V} \times (\nabla \times \mathbf{V}) \right] \\ &= -\nabla P - \mathbf{1}_z \times \mathbf{V} + Ra \Pi_z + E\Delta \mathbf{V}, \quad (1) \\ & \frac{\partial T}{\partial t} + (\mathbf{V} \cdot \nabla)(T + T_0) = \Delta T. \end{aligned}$$

The dimensionless numbers of Prandtl, Ekman, Rayleigh, and Roberts are introduced as $Pr = \frac{\nu}{\kappa}$, $E =$

$$\frac{\nu}{2\Omega L^2}, \text{ and } Ra = \frac{\alpha g_0 \delta T L}{2\Omega \kappa},$$

where ν is the coefficient of kinematic viscosity, α is the coefficient of volumetric expansion, g_0 is the free fall acceleration, δT is the unit of temperature disturbance (T) relative to the “diffusion” temperature distribution $T_0 = 1 - z$, and η is the coefficient of magnetic diffusion. We introduce the Rossby number as $Ro = EPr^{-1}$. The problem (1) was solved in a rectangular box with the periodic boundary conditions along coordinates x and y . For the $z = 0$ and 1 boundaries, temperature disturbances are zero, which is equivalent to the specification of temperature at the $\tilde{T} = T + T_0 = 1$ and 0 boundaries (heating from below), if the selected T_0 profile is taken into account. For the velocity field, we accept the condition of impenetrability and equality to zero of the tangential component gradients at $z = 0$ and 1 : $V_z =$

$$\frac{\partial V_x}{\partial z} = \frac{\partial V_y}{\partial z} = 0.$$

Such a statement of the boundary conditions guarantees that the tangential components of the viscous stress tensor and the values of hydrodynamic helicity are zero. To solve (1), we used the pseudospectral code (for more detail, see [Orszag, 1971; Meneguzzi and Pouquet, 1989; Cattaneo et al., 2003]), adapted for parallel processes using MPI [Reshetnyak, 2007]. The calculations were performed using the N^3 grid ($N = 64$).

3. FLUXES IN k SPACE

The concept of fluxes in the wave space can be considered in more detail in [Frisch, 1995; Reshetnyak, 2008] and references therein. To describe exchange interactions in the Fourier space, it is convenient to divide the wave space into such shells that $k_i < k < k_{i+1}/k_i = \gamma$ (it is usually accepted that $\gamma = 2$). We will subsequently be interested in the energy exchange between such shells (cascade processes). We introduce the field f expansion into the HF and LF components: $f(\mathbf{r}) = f^<(\mathbf{r}) + f^>(\mathbf{r})$, where

$$f^<(\mathbf{r}) = \sum_{|k| \leq K} \hat{f}_k e^{i\mathbf{k}\mathbf{r}}, \quad f^>(\mathbf{r}) = \sum_{|k| > K} \hat{f}_k e^{i\mathbf{k}\mathbf{r}}, \quad (2)$$

respectively. For the periodic fields f and g , we have (for more detail, see [Frisch, 1995]):

$$\left\langle \frac{\partial f}{\partial x} \right\rangle = 0, \quad \left\langle g \frac{\partial f}{\partial x} \right\rangle = -\left\langle f \frac{\partial g}{\partial x} \right\rangle, \quad \langle f^> g^< \rangle = 0, \quad (3)$$

where

$$\langle f(\mathbf{r}) \rangle = V^{-1} \int_V f(\mathbf{r}) d\mathbf{r}^3 \quad (4)$$

means averaging of field f over volume V . Multiplying the Navier–Stokes equation into \mathbf{V}^ζ , we have the expression for a change in the kinetic energy in a sphere with radius K , average over a volume:

$$\begin{aligned} 2^{-1} \text{EPr}^{-1} \left[\frac{\partial \langle V_i^\zeta V_i^\zeta \rangle}{\partial t} + \Pi(K) \right] \\ = \text{Ra} \langle T^\zeta V_z^\zeta \rangle - \text{E} \langle (\nabla \omega^\zeta)^2 \rangle, \end{aligned} \quad (5)$$

where the kinetic energy integral flux from the $k > K$ region into the $k \leq K$ region is specified in the form

$$\Pi(K) = \langle V_i^\zeta \cdot (V_j \cdot \nabla_j) V_i \rangle, \quad (6)$$

and summation is taken with respect to the repeated indices $i = 1, \dots, 3$. It is convenient to introduce the kinetic energy local flux T_k :

$$T_K(k) = -\frac{\partial \Pi(k)}{\partial k}, \quad \int_{k=0}^{\infty} T_K(k) dk = 0. \quad (7)$$

In such a case, we have the following expression for the Navier–Stokes equation:

$$\frac{\partial E(k)}{\partial t} = T_K(k) + F(k) + D(k), \quad (8)$$

where $E(k) = \frac{1}{2} \frac{\partial}{\partial k} \langle \mathbf{V}_k^2 \rangle$ is a change in the kinetic

energy at wavenumber k , $F(k) = \frac{\text{RaPr}}{\text{E}} \frac{\partial}{\partial k} (TV_z^\zeta)$ is the

work of the buoyancy force, and $D(k) = -\text{Pr}k^2 E(k)$ is dissipation. Expression (8) describes the kinetic energy total flux via wavenumber k .

To study the detailed structure of the triad mechanism, we can determine the form of the energy equation describing energy transfer from shells Q and P to shell K :

$$\frac{\partial E(K)}{\partial t} = T_3 + A(K) + D(K), \quad (9)$$

where $E(K)$ and $D(K)$ have the same form as in (8), $T_3 = \langle V_i(K) \cdot (V_j(P) \cdot \nabla_j) V_i(Q) \rangle$, and $A(K) = \frac{\text{RaPr}}{\text{E}} \langle T(K) V_z(K) \rangle$.

It is also useful to introduce the $T_2(K, Q) = \int T_3(K, Q, P) dP$ function. Generally speaking, the latter should be explained. We can demonstrate that T_2 means the energy flux from harmonic Q to harmonic K (see references in [Alexakis et al., 2007]). An analysis of T_2 makes it possible to estimate whether the energy

transfer is local or not rather than the locality of the interaction itself. Studying T_3 makes it possible to completely restore the wave triangle structure and to elucidate whether the interaction itself is local or not. Note also the useful properties of function T_2 : in the general case for arbitrary periodic (or random homogeneous) nondivergent fields $\mathbf{u}(Q)$, $\mathbf{w}(K)$, and \mathbf{V} , we have [Alexakis et al., 2005] $T_2^{uw}(Q, K) = -T_2^{wu}(K, Q)$,

where $T_2^{uw}(Q, K) = \langle u_i(K) \cdot (V_j \cdot \nabla_j) w_i(Q) \rangle$, and $T_{wu}(Q, K) = \langle w_i(Q) \cdot (V_j \cdot \nabla_j) u_i(K) \rangle$, which corresponds to the equality between the energies received by shell K from shell Q and transferred from shell Q to shell K . In the following section, we will consider the properties of fluxes T_K , T_2 , and T_3 , using set (1) as an example, and will elucidate how these fluxes change when rotation is introduced.

4. FIELD SPECTRA AND ENERGY TRANSFER DIRECTION

We now briefly consider the results of [Reshetnyak, 2008], which is necessary for us to understand the following material, and will subsequently consider the problem of locality of the triad interaction and energy transfer.

We consider three convection regimes.

NR: the regime without convection (the Coriolis force is zero); $\text{Ra} = 9 \times 10^5$, $\text{Pr} = 1$, $\text{E} = 1$, and $\text{Re} \sim 700$.

R1: the regime with rotation; $\text{Ra} = 4 \times 10^2$, $\text{Pr} = 1$, $\text{E} = 2 \times 10^{-5}$, and $\text{Re} \sim 200$.

R2: the regime with rotation; $\text{Ra} = 1 \times 10^3$, $\text{Pr} = 1$, $\text{E} = 2 \times 10^{-5}$, and $\text{Re} \sim 10^4$.

These regimes correspond to convection close to Kolmogorov convection (NR) and geostrophic convection (R1 and R2). Subsequently, we will omit the description of the flux morphology considered in [Reshetnyak, 2007, 2008] and will study the kinetic energy fluxes in the wave space.

The NR regime corresponds to turbulent convection without rotation. The spectral properties of convection are close to the Kolmogorov dependence $\sim k^{-5/3}$ (Fig. 1), and the amplitude of the kinetic energy chaotic oscillations accounts for $\sim 15\%$ of the average energy level.

Thermal convection with rotation is characterized by the appearance of many vertically rotating columns (cyclones–anticyclones). The number of these columns depends on the Ekman number as $k_c \sim \text{E}^{-1/3}$ [Chandrasekhar, 1961; Busse, 1970; Jones and Roberts, 2000]. For the Earth’s liquid core, $\text{E} \sim 10^{-15}$, which does not evidently make it possible to perform calculations at realistic values of the parameter. One usually manages to reach regimes with $\text{E} = 10^{-4} - 10^{-6}$ [Jones, 2000]. The aim of numerical experiments is to

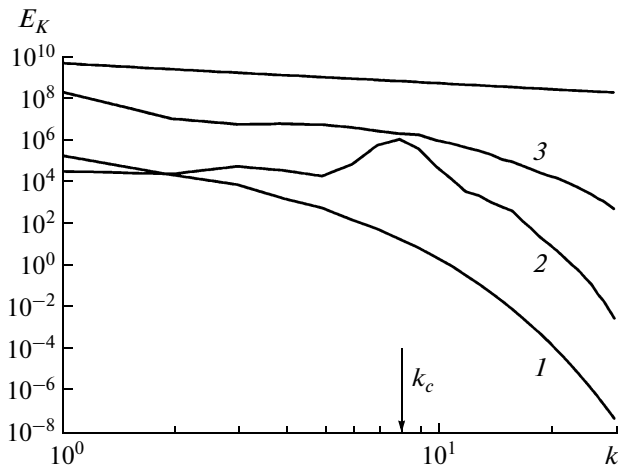


Fig. 1. Kinetic energy spectra for the NR (1), R1 (2), and R2 (3) regimes. A straight line corresponds to the $\sim k^{-5/3}$ Kolmogorov spectrum.

obtain an asymptotic regime and to perform the corresponding interpolation to the Earth's parameters. A linear analysis also indicates that the critical Rayleigh number, at which convection begins, depends on the Ekman number as $Ra^{cr} \sim E^{-1/3}$. An increase in Ra^{cr} is related to the appearance of cyclonic convection, resulting in increased dissipation.

The R1 regime corresponds to the geostrophic convection state near the generation threshold, which is characterized by the regular spatial structure of cyclones. An increase in Ra (regime R2) results in a disturbance of cyclone ordering, appearance of small-scale fluxes in the z direction, and deviation from the geostrophic state. The spectra of convection with rotation differ from the regime without rotation (Fig. 1). Regime R1 is close to the threshold regime. A peak ($k_c \sim 8$) corresponding to cyclonic flows is clearly defined in the integral spectrum (the upper curve). With increasing Ra (regime R2), a spectrum notch is filled, and the integral spectrum becomes similar to the spectrum without rotation.

The observed similarity in the behavior of the R2 and NR spectra does not yet indicate that the physical processes are similar: it is known that the kinetic energy spectrum $\sim k^{-5/3}$ is also observed in two-dimensional turbulence [Kraichnan and Montgomery, 1980], but the energy is transferred from small scales to large ones rather than in the opposite direction. The presented estimates of the terms for R2 [Reshetnyak, 2008] indicate that the geostrophic balance is satisfied.

We now consider the behavior of $T_K(k)$. The NR regime demonstrates the known pattern of a Kolmogorov direct kinetic energy cascade (Fig. 2). For large scales, $T_M^< 0$: these scales are energy sources. When we go to the IR spectrum, the flux sign reverses: the energy is consumed. For two-dimensional turbulence,

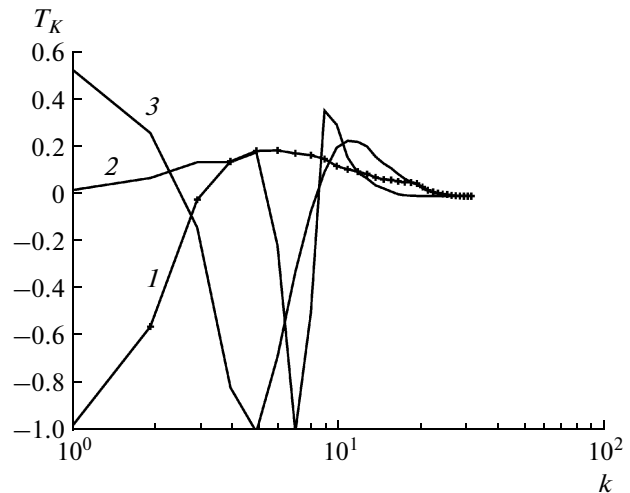


Fig. 2. Kinetic energy fluxes $T_K(k)$ for the NR (1), R1 (2), and R2 (3) regimes.

a twin pattern of the flux is observed [Kraichnan and Montgomery, 1980]. In this case an inverse cascade is observed instead of a direct cascade.

Rotation substantially changes the behavior of energy fluxes. The energy is carried by the wavenumber k_c . For $k > k_c$, we also observe a direct energy cascade $T_K^< > 0$. A shift of the $T_K^<$ maximum to the right relative to the spectral maximum increases with increasing Re . For $k < k_c$, the pattern is substantially more complex: an inverse energy cascade ($T_K^< > 0$) is observed for large wavenumbers.

5. ENERGY FLUX LOCALITY

We now consider the structure of triad interactions. Figure 3 presents the diagram of the T_2 fluxes antisymmetric about the $K = Q$ diagonal for the regimes considered above. The pattern generally resembles the results with forcing (see [Alexakis et al., 2007]: harmonics with $K > Q$ take the energy from harmonics with $K < Q$ (direct energy cascade). The flux maximum falls on harmonics with $K \sim Q$ close to the diagonal; i.e., the energy being locally transferred. Note that in some regions (e.g., $Q = 5$, $K = 20$) a nonlocal inverse cascade is also observed (see the discussion in the Introduction); however, the integral pattern is close to the idealized Kolmogorov scenario. It is convenient to represent the diagram shown in Fig. 3 in the form of an integral over Q and K as a $K-Q$ function (see Fig. 4). Figure 4 distinctly demonstrates that a direct cascade and local interaction and energy transfer are present.

Rotation changes the behavior of T_2 for $k < k_c$, remaining this temperature almost unchanged for the HF region ($k > k_c$). We now consider the appeared changes in more detail. The absolute maximums

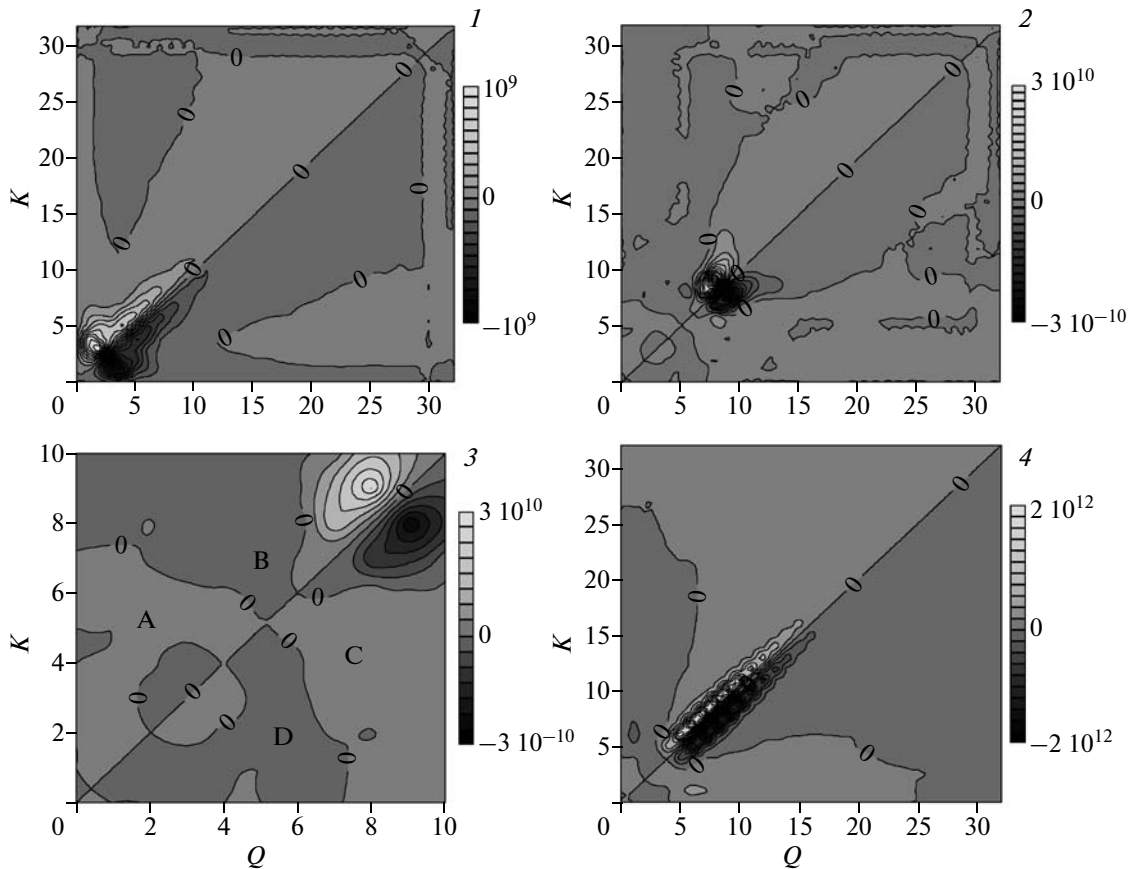


Fig. 3. Kinetic energy fluxes $T_2(k)$ for the NR (1), R1 (2 and 3), and R2 (4) regimes.

(minimums) are located in the region close to k_c ; i.e., the energy being transferred from a leading mode into the region with large k . On the other hand, the energy flux sharply decreases for $k < k_c$, which corresponds to an approach of the system to the statistical equilibrium that is also observed in Fig. 2. A finer structure is observed for small k in the enlarged image (see Fig. 3, panel 3): region A with a direct energy cascade but with an equiprobable energy transfer from small $Q \sim K$ and from relatively large $Q \sim 4K$. Region B with an inverse energy cascade (and a small energy flux amplitude that accounts for about 1/10 of the absolute maximum as in region A) has an extended strip shape from $Q \sim K$ to $Q \sim 10K$. This corresponds to the appearance of a small negative maximum for $K > Q$ in Fig. 4.²

An increase in Ra (regime R2) results in a shift of the region with an inverse energy cascade toward small Q and $K > Q$. As before, we can speak about the existence of the state, which is close to a homogeneous distribution for $k < k_c$. This regime is also characterized by a longer interval in the $k > k_c$ region with a local energy transfer and direct cascade. The relative contri-

bution of the region with inverse cascade decreases (see Fig. 4, plot 3). At the same time, this contribution shifts to the large-scale region $k \ll k_c$, which can be of interest for the geodynamo problems, when the distance between $k_c \sim 10^5$ and the region of magnetic field generation is at least several orders of magnitude (at present-day estimates of the magnetic Reynolds number $R_m \sim 10^2 - 10^3$, the region of magnetic field generation lies in the $k \sim 1 - 10^3$ range).

6. INTERACTION LOCALITY

We consider in more detail the properties of the T_3 function for the regimes considered above. For reasons of symmetry, we anticipate that $T_3(K, P, Q) = T_3(K, Q, P)$, which was used to construct a discrete analog for an operator. The case without rotation (Fig. 5, panels 1, 2) demonstrates an extremely interesting result: the contribution of two sources (waves with $P \leq K, Q \ll P$ and $Q \leq K, P \ll Q$) to the energy flux, which falls on harmonic K , is maximal. In other words, a wave triangle is oblique and has a small angle between equal sides K, P or K, Q . Taking into account the fact that the energy is transferred to K from the nearest smallest wavenumber according to Fig. 4, we can

² We do not comment the behavior of the curve for $K < Q$ (regions C and D) since this plot is antisymmetric.

arrive at the conclusion that the third vector with a small amplitude is a catalyst. When participating in the exchange process, this HF harmonic does not transfer the energy to wave K . The result is beyond the classical Kolmogorov theory, according to which a wave triangle should be oblique; i.e., not only the energy transfer being local but also the triad interaction shows this property. This is caused by two factors. First, taking into account the data obtained by Alexakis et al. [2007], we relate this to an insufficient length of the considered spectrum since we have only several vertical plumes for the resolution used in the NR regime. On the other hand, we relate this to the existence of plumes themselves and, consequently, to the system anisotropy. In this connection, it is known that the flux anisotropy on small scales is substantial even at substantially larger Reynolds numbers in the problems with forcing [Zhou and Yeung, 1996]. Our simulation indicates that the energy fluxes on small scales highly correlate with the buoyancy force on a large scale. This is demonstrated by the behavior of the function $r(K) = \int T_3 \max(P/Q, Q/P) dPdQ / \int T_3 dPdQ$ ($P, Q > 0$), see Fig. 6. The angle $\alpha(K) = \int T_3 dPdQ / \int T_3 dPdQ$ ($f = (P^2 + Q^2 - K^2)/2PQ$) between the \mathbf{p} and \mathbf{q} vectors is about 100° for almost all K ; i.e., the modes that participate in the interaction being close to the orthogonal modes in the wave space.

We now consider the case with rotation. The triad structure for small Ra strongly differs from this structure in the regime without rotation. The same harmonic interacts with the entire wave packet: the diagram is cruciform. The latter is possible due to an increase in the angle between the \mathbf{p} and \mathbf{q} vectors. Note that $P \sim Q$ for small K and P (see Fig. 6). An inverse energy cascade for small K is clearly defined in Fig. 5: the harmonic with $K = 7$ obtains the energy from large wavenumbers and transfers this energy to the HF spectral region. As K increases, we approach again the state when $P \sim Q$ and $\alpha \sim 100^\circ$. However, in contrast to the case without rotation, the energy of wave K is transferred from waves with $P \sim Q \approx 0.7 K$. When Ra increases, the system starts operating in the intermediate regime between the regimes considered above.

7. DISCUSSION AND CONCLUSIONS

We now consider the main results of the work. Rotation substantially changes the morphology and spectral composition of the fluxes in the physical space. The position of the system in the wave space strongly differs from such a position of a leading mode k_c even for relatively small amplitudes of thermal sources. For modes with $k < k_c$, an insignificant inverse cascade is observed, and the interaction becomes non-local. For modes with $k > k_c$, an energy cascade becomes direct; however, a nonlocal energy transfer is possible from small $k \sim k_c$. The aforesaid can be the

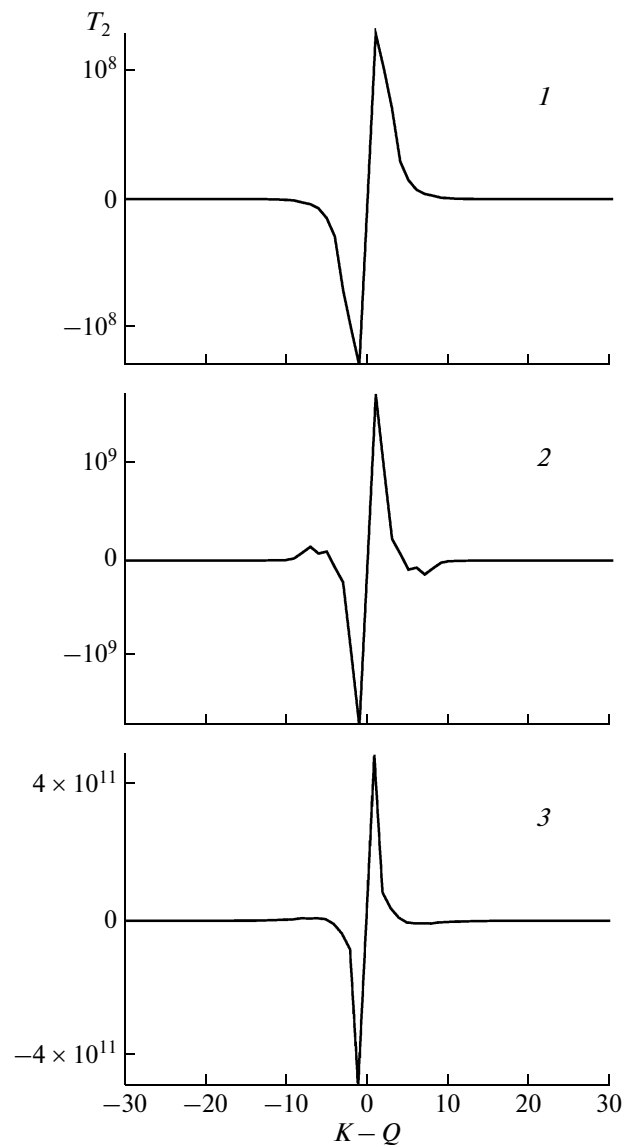


Fig. 4. Kinetic energy fluxes $T_2(K - Q)$ for the NR (1), R1 (2), and R2 (3) regimes.

motivation for the development of low-mode models of turbulence with an energy source at k_c .

The approaches considered above demonstrate a diverse interaction between individual modes in a still rather simple (from the standpoint of a complete geodynamo problem) system without magnetic field. Such an analysis will make it possible to tune the developed models with turbulent coefficients of transfer so that the flux values for scales larger than the averaging scale (d_a) would coincide with the values considered above during the direct numerical simulation. Only such a step-by-step comparison can guarantee the accurateness of the introduced semiempirical model of turbulence. It is nontrivial to represent an inverse energy cascade in the case when $d_c < d_a$.

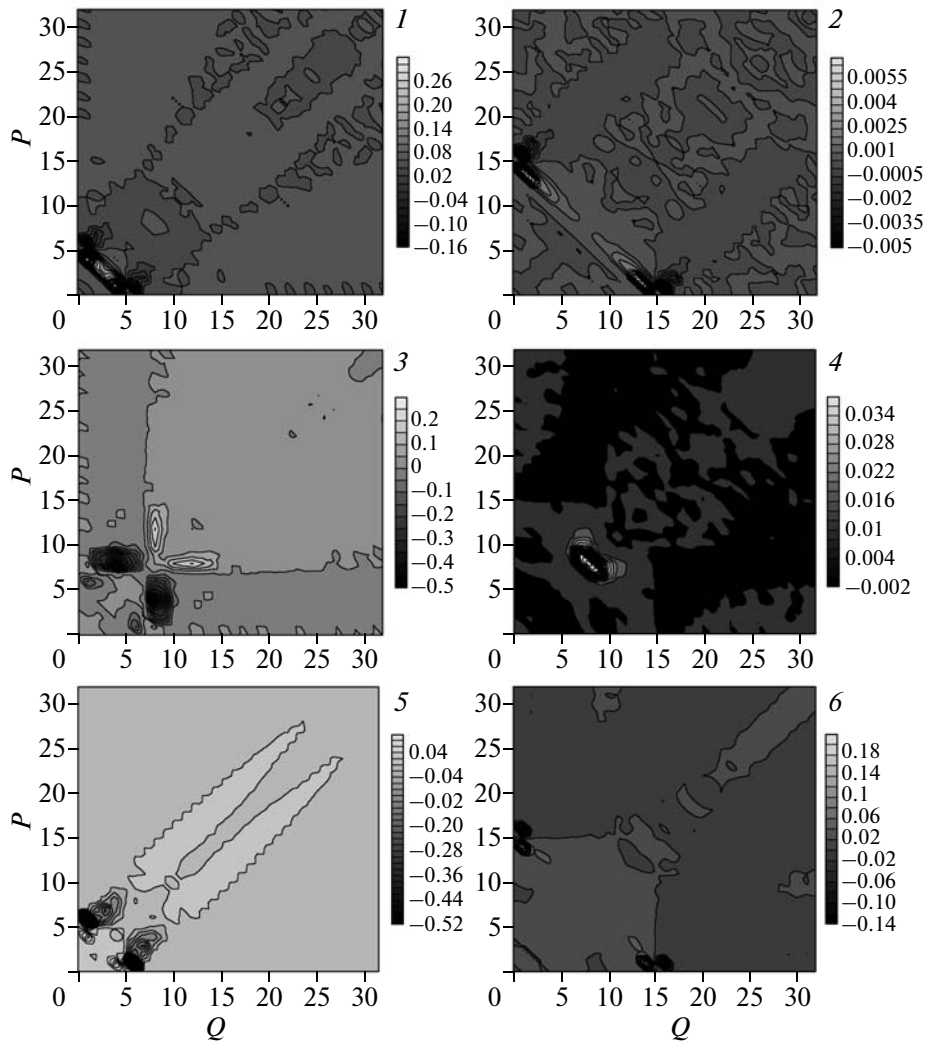


Fig. 5. Amplitudes of T_3 fluxes for fixed k . NR: $k = 5$ (1) and 15 (2); R1: $k = 7$ (3) and 15 (4); R2: $k = 5$ (5) and 15 (6). The values are normalized to the maximal flux values for all P , Q , and K .

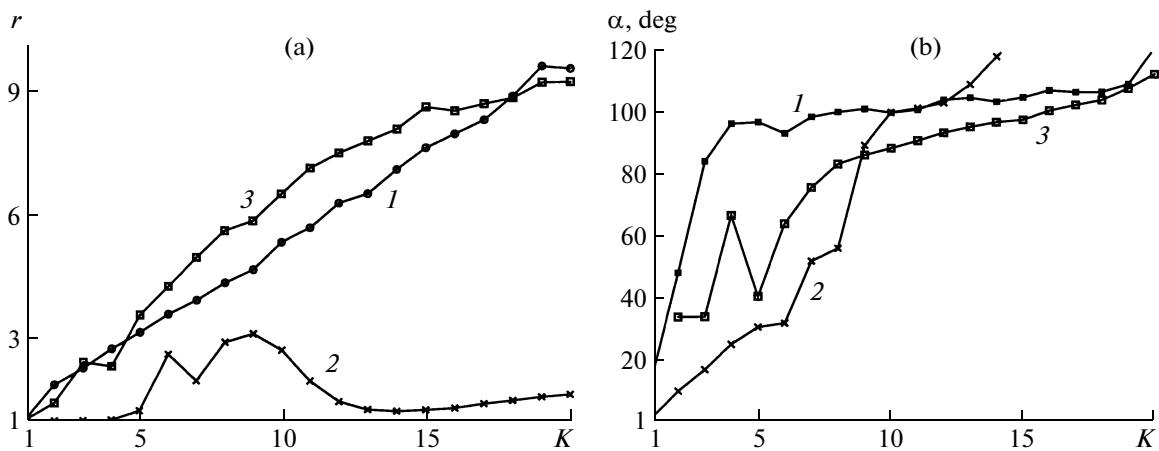


Fig. 6. Variations in the P/Q and Q/P wavenumber ratio maximums (panel a) and the angle between the \mathbf{p} and \mathbf{q} vectors (panel b), entering into the triad interaction, vs. the wavenumber (K) of the resultant harmonic.

ACKNOWLEDGMENTS

This work was supported by the Russian Foundation for Basic Research, project no. 03-05-64074.

REFERENCES

- A. Alexakis, P. D. Mininni, and A. Pouquet, "Shell to Shell Energy Transfer in MHD. I. Steady State Turbulence," *Phys. Rev. E* **72**, 046301–046309 (2005).
- A. Alexakis, P. D. Mininni, and A. Pouquet, "Turbulent Cascades, Transfer, and Scale Interactions in Magneto-hydrodynamics," *New J. Phys.* **298** (9), 1–20 (2007).
- F. H. Busse, "Thermal Instabilities in Rapidly Rotating Systems," *J. Fluid Mech.* **44**, 441–460 (1970).
- F. Cattaneo, T. Emonet, and N. Weis, "On the Interaction between Convection and Magnetic Fields," *ApJ* **588**, 1183–1198 (2003).
- S. Chandrasekhar, *Hydrodynamics and Hydromagnetic Stability* (Dover Publ. Inc., New York, 1981).
- P. Constantin, "Energy Spectrum of Quasigeostrophic Turbulence," *Phys. Rev. Lett.* **89** (18), 184501-1–184501-4 (2002).
- U. Frisch, *Turbulence: The Legacy of A. N. Kolmogorov* (Cambr. Univ. Press, Cambridge, 1995; Fizis, Moscow, 1998).
- M. Hossain, "Reduction in the Dimensionality of Turbulence Due to a Strong Rotation," *Phys. Fluids* **6** (4), 1077–1080 (1994).
- C. A. Jones and P. H. Roberts, "Convection Driven Dynamos in a Rotating Plane Layer," *J. Fluid Mech.* **404**, 311–343 (2000).
- C. A. Jones, "Convection-Driven Geodynamo Models," *Philos. Trans. R. Soc. (London)*, A **358**, 873–897 (2000).
- R. H. Kraichnan and D. Montgomery, "Two-Dimensional Turbulence," *Rep. Prog. Phys.* **43**, 547–619 (1980).
- F. Krause and K.-H. Rädler, *Mean Field Magnetohydrodynamics and Dynamo* (Akademie-Verlag, Berlin, 1980; Mir, Moscow, 1984).
- M. Lesieur, *Turbulence in Fluids* (Kluwer Acad. Publ., Netherlands, 1990).
- W. D. McComb, *The Physics of Fluid Turbulence* (Clarendon Press, Oxford, 1992).
- M. Meneguzzi and A. Pouquet, "Turbulent Dynamos Driven by Convection," *J. Fluid Mech.* **205**, 297–318 (1989).
- S. A. Orszag, "Numerical Simulation of Incompressible Flows within Simple Boundaries. I. Galerkin (Spectral) Representations," *Stud. Appl. Math.* **L** (51), 293–327 (1971).
- J. Pedlosky, *Geophysical Fluid Dynamics* (Springer, New York, 1987).
- M. Yu. Reshetnyak, "Certain Spectral Properties of Cyclonic Turbulence in the Earth's Liquid Core," *Geomagn. Aeron.* **48** (3), 416–423 (2008) [*Geomagn. Aeron.* **48**, 400–407 (2008)].
- M. Yu. Reshetnyak, "Thermal Convection and Dynamo during Rapid Rotation," *Fiz. Zemli*, No. 8, 23–32 (2007).
- Y. Zhou and P. K. Yeung, "Scale Disparity and Spectral Transfer in Anisotropic Numerical Turbulence," *Phys. Rev. E* **53**, 1261–1264 (1996).
- Y. Zhou, "A Phenomenological Treatment of Rotating Turbulence," *Phys. Fluids* **7** (9), 2092–2094 (1995).